Proceedings of the 17th Pan-American Conference on Soil Mechanics and Geotechnical Engineering (XVII PCSMGE), and 2nd Latin-American Regional Conference of the International Association for Engineering Geology and the Environment (IAEG), La Serena Chile, 2024.

Role of mineralogy in the biocementation of soils in geotechnical engineering.

Rol de la mineralogía en la biocementación de suelos en la ingeniería geotécnica.

[Victoria] [Meza - Ochoa]
[Facultad de ingeniería], [Politécnico Colombiano Jaime Isaza Cadavid], [Medellín, Colombia], [vemeza@elpoli.edu.co]

[Marco Antonio] [Márquez - Godoy] & [Hernán] [Martínez - Carvajal]
[Facultad de Minas], [Universidad Nacional de Colombia], [Medellín, Colombia]

ABSTRACT: In recent decades, biogeotechnology has emerged as a sustainable alternative for solving various problems in geotechnical engineering, through the study and application of biological and microbiological processes, reactions and mechanisms. Microbially Induced Calcium Carbonate Precipitation (MICP) has proven to be a highly efficient process for biocementing fine sands, primarily composed of quartz. To biocement soils with diverse mineralogical composition, this study evaluated the influence of mineralogy on MICP in silica sands (SS), kaolin (KC) and bentonite clays (BC), treated with commercially available strains of *Sporosarcina pasteurii*, *Sutcliffiella cohnii* and *Corynebacterium ammoniagenes*. The experimental investigation was conducted at different laboratory scales. In the Erlenmeyer flask tests, the results demonstrated the effectiveness of *Sporosarcina pasteurii* as the most suitable microorganism for MICP in the soil. The behavior of the pH, dissolved oxygen, and concentration of calcium in solution was influenced by the different substrates, as well as the polymorph and the amount of precipitated calcium carbonate (CC). In larger-scale experiments, the biocementation of soil cylinders of 100% SS, blend of 90% SS - 10% KC, and mix of 90% SS - 10% BC, was achieved using *Sporosarcina pasteurii*. Scanning Electron Microscopy (SEM) results revealed that calcium carbonate particles (principally vaterite) with a spherical habit, precipitate in the soil matrix, creating contact bridges between the coarse quartz particles and forming agglomerations on the surface of the particles. The Unconfined Compressive Strength (UCS) of the 100% SS and 90% SS-10% KC was 934 kPa and 96 kPa, respectively. The 90% SS-10% BC did not achieve complete cementation and USC could not be determined. It is considered that the presence of CC in the BC substrate and the smaller particles generating a larger surface area (montmorillonite) may have favored the precipitation of CC and specific calcite formation. Moreover, the presence of montmorillonite per se catalyzes CC nucleation.

KEYWORDS: Biocementation, biomineralization, calcium carbonate precipitation, MICP, soil mineralogy

RESUMEN: En las últimas décadas, la biogeotecnología ha surgido como una alternativa sostenible para resolver diversos problemas en la ingeniería geotécnica, mediante el estudio y aplicación de procesos, reacciones y mecanismos biológicos y microbiológicos. La Precipitación de Carbonato de Calcio Inducida Microbiológicamente (MICP) ha demostrado ser un proceso altamente eficiente para la biocementación de arenas finas, principalmente compuestas por cuarzo. Con el fin de biocementar suelos con una composición mineralógica diversa, este estudio evaluó la influencia de la mineralogía en la MICP en arenas de sílice (SS), caolín (KC) y arcillas de bentonita (BC), tratadas con cepas comercialmente disponibles de *Sporosarcina pasteurii, Sutcliffiella cohnii* y *Corynebacterium ammoniagenes*. La investigación experimental se llevó a cabo en diferentes escalas de laboratorio. En los ensayos con Erlenmeyer, los resultados demostraron la efectividad de la *Sporosarcina pasteurii* como el microorganismo más adecuado para la MICP en el suelo. El comportamiento del pH, oxígeno disuelto y concentración de calcio en solución fue influenciado por los diferentes sustratos, de la misma manera, el substrato mineral tuvo influencia en el polimorfo y la cantidad de carbonato de calcio precipitado (CC). En experimentos a mayor escala, se logró la biocementación de cilindros de suelo compuestos por 100% SS, mezcla de 90% SS - 10% KC y mezcla de 90% SS - 10% BC, utilizando *Sporosarcina pasteurii.* Los resultados de Microscopía Electrónica de Barrido (SEM) revelaron la existencia de partículas de carbonato de calcio (principalmente vaterita) con una morfología esférica precipitando en la matriz del suelo, creando puentes de contacto entre las partículas gruesas de cuarzo y formando aglomeraciones en la superficie de las partículas. La resistencia a la compresión no confinada (UCS) de los cilindros de 100%SS y 90% SS-10% KC fue de 934 kPa y 96 kPa, respectivamente. La muestra de 90% SS-10% BC no logró una cementación completa y no se pudo determinar el UCS. Se considera que la presencia de CC en el sustrato de BC y las partículas más pequeñas que generan una mayor área superficial (montmorillonita) pueden haber favorecido la precipitación de CC y la formación específica de calcita. Adicionalmente, la presencia de montmorillonita per se cataliza la nucleación de CC.

PALABRAS CLAVE: biocementación, biomineralización, precipitación de carbonato de calcio, MICP, mineralogía del suelo

1 INTRODUCTION.

In recent decades, biogeotechnology has emerged as a sustainable alternative for addressing various challenges in geotechnical engineering. Microbially Induced Calcium Carbonate Precipitation (MICP) is one such process that has been explored in various geotechnical contexts for its effectiveness in modifying and enhancing the engineering properties of soils.

MICP is a process of induced biomineralization, where the microorganism (calcifying bacteria) creates optimal conditions within the local microenvironment to enable extracellular chemical precipitation of mineral phases (Hamilton 2003), specifically calcium carbonate ($CaCO_3$). This precipitation occurs in an environment oversaturated with dissolved calcium ions (Ca^{2+}) and bicarbonates (H_2CO_3) resulting from the hydrolysis of urea, as illustrated by Eq. 1 and Eq. 2 (36, 44).

$$CO(NH_2)_2 + 2H_2O \rightarrow 2NH_4^+ + CO_3^{2-} \qquad (1)$$

$$Ca^{2+} + CO_3^{2-} \rightarrow CaCO_3 \qquad (2)$$

MICP has demonstrated its efficacy in reducing soil expansion potential and mitigating or diminishing sand liquefaction potential (DeJong et al. 2006, Ivanov & Chu 2008;). Furthermore, MICP has shown promise in enhancing load-bearing capacity, slope stability, facilitating tunnel excavation (Whiffin et al. 2007, Van Paassen 2009), and controlling erosion in coastal or river areas (Ivanov & Chu 2008), among other applications.

Biocementation involves the selective deposition of $CaCO_3$ crystals at soil inter-particle contacts, forming cementing bonds between the particles (Ivanov & Chu 2008). These bonds effectively enhance the strength and stiffness of the soil. The biocementation process has been particularly efficient for fine sands, predominantly composed of quartz. However, the role of soil mineralogy on MICP is a critical aspect influencing the success of soil improvement and stabilization. Soil mineralogy can affect the availability of calcium ions, pH levels, and the growth and metabolic activities of calcifying bacteria, ultimately affecting the degree of calcium carbonate precipitation and soil strengthening.

To address biocementation in soils of diverse mineralogical composition, this study evaluates the influence of mineralogy on MICP in silica sands (SS), kaolin (KC) and bentonite clays (BC), treated with commercially available strains of *Sporosarcina pasteurii*, *Sutcliffiella cohnii* and *Corynebacterium ammoniagenes*

2 MATERIALS AND METHODS.

2.1 *Used soils*

Three types of soils were used in the study: silica sand (SS) provided by Antioqueña de Arenas S.A.S of Colombia, kaolin (KC) sourced from Sumicol S.A.S, and bentonite clay (BC) supplied by Protokimica S.A.S. These soils were selected as representative mineral substrates of quartz (silica sand), kaolinite (kaolin) and montmorillonite (bentonite clay), which are predominant in each soil.

2.2 *Characterization of untreated soils*

Moisture content (w%), specific gravity (Gs), consistency limits, and granulometry by sieving were determined according to the ASTM D2216-10, 854-14, 4318-17, 6913-17 standards, for subsequent classification according to the Unified Soil Classification System - USCS (ASTMD 2487-17).

The pH was measured and the exchangeable cations Ca^{2+}, Mg^{2+}, Na^+, K^+ were determined using the ammonium acetate extraction method at pH 7 and atomic absorption titration (NTC 5349-2016).

Mineralogical characteristics were determined using Fourier Transform Infrared Spectroscopy (FTIR), employing the transmission method. A wavenumber interval between 400 and 4000 cm^{-1} and 48 scans were utilized.

2.3 *Microorganism and culture media*

MICP in the mineral substrates was induced using the urease-positive bacteria *Sporosarcina pasteurii* (DSMZ 323), *Sutcliffiella cohnii (Bacillus cohnii)* (DSMZ 6307) and *Corynebacterium ammoniagenes* (DSMZ 20306). These were cultivated in a medium composed of: 20 g/l of yeast extract, 10 g/l of ammonium chloride (NH_4Cl) and 10 μM of nickel chloride ($NiCl_2$) (Van Paassen 2009) maintained at temperature of 30 ºC, in an orbital shaker at 140 rpm (revolutions per minute), until it reached a bacterial concentration of 10^8 cells/ml. All the components of the culture media were previously sterilized in an autoclave at 121 ºC.

2.4 *Cementation reagent*

The cementation reagents added to the culture media were urea and calcium chloride, forming an equimolar solution at a concentration of 0.25 M in the Erlenmeyer scale tests and 0.50 M in the soil cylinders. Calcium chloride was previously sterilized in an autoclave at 121 ºC and the urea was filtered through a cellulose membrane of 0.2 μm (Whiffin 2004).

2.5 *Calcium carbonate (CC) precipitation bioassay*

The experiment on biomineralization for calcium carbonate (CC) precipitation was conducted in Erlenmeyer flasks. A suspension was formed with a weight ratio of 1:10, consisting of 20 g of mineral substrate and 200 ml of liquid medium. The liquid medium was composed of 100 ml of culture media, 10 ml of bacterial inoculum and 90 ml of cementing reagents at a concentration of 0.25 M. The initial pH of the solution was adjusted to 8.5. Additionally, a negative control was prepared without bacterial inoculum.

The bioassays and controls were carried out by shaking the flasks at 100 rpm and maintaining a temperature of 30°C for 15 days. At defined intervals (2h, 4h, 24h, 3, 6, 9, 12 and 15 days), 10 ml of the solution were taken from each experiment to monitor changes in pH, dissolved oxygen (DO), and calcium (Ca^{2+}) concentration in the solution. The pH and DO were measured using a multiparameter device, while calcium measurements were performed using an Inductively Coupled Plasma - Mass Spectrometry (ICP-MS) with an Agilent 4100 mass spectrometer.

At the conclusion of the biomineralization experiment, Fourier Transform Infrared Spectroscopy (FTIR) analyses were conducted on the samples to identify the presence of CC and its polymorphs. To quantify the CC in the soils, the method of soil mass loss through the dissolution of carbonates with hydrochloric acid 1M was used (Lee, Ng & Tanaka 2013).

2.6 *Biocemented soils by MICP*

To verify the feasibility of cementing soils with different mineralogy using MICP, soil samples of 5 cm in diameter and 12 cm in height were prepared, with a dry density of 12 kN/m^3. Cylindrical acrylic molds, 20 cm in height were utilized, and the soils were placed into the molds by gravity, slightly vibrated. The biotreatment was administered using a peristaltic pump with downward flow (see Figure 1).

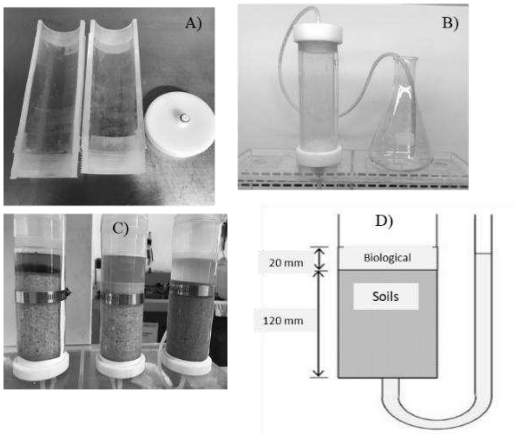

Figure 1. Set up soil biocementation tests. a) Acrylic mold divided in half. b) Mold closed and placed in a vertical position. c) Soils in the cylindrical acrylic molds. d) Assembly diagram.

Three soils were prepared, consisting of 100%SS, a blend of 90%SS -10%KC and a mix of 90%SS -10%BC (refer to Table 1). These soils were subjected to four successive MICP treatments, each with a retention time of 48 h. The treatment procedure involved immersing the soil and saturating it in a liquid medium composed of 40% culture medium, 10% bacterial inoculum and, 50% cementing reagents at a concentration of 0.5M.

After 48 h of each treatment, the calcium concentration in the solution was measured. At the end of the bioassay, the soils were air-dried and mineralogical characterization was conducted using FTIR and Scanning Electron Microscopy with Energy Dispersive X-ray Spectroscopy (SEM-EDX) analysis. These analyses aimed to identify morphological and textural relationships between the soils and precipitated CC. SEM images were performed using secondary electron (SE) and backscatter electron (BSE) observation modes.

Table 1. Soil samples subjected to biological treatment MICP

#	Code	*Sample*
1	*S.p*-SS	*S. pasteurii* and 100% SS
2	*S.p*-SS:KC10	*S. pasteurii* and 90% SS -10% KC
3	*S.p*-SS:BC10	*S. pasteurii* and 90% SS -10%BC
4	*B.c*-SS	*S. cohnii* and 100% SS
5	*B.c*-SS:KC10	*S. cohnii* and 90% SS-10% KC
6	*B.c*-SS:BC10	*S. cohnii* and 90% SS -10% BC
7	*C.a*-SS	*C. ammoniagenes* and 100% SS
8	*C.a*-SS:KC10	*C. ammoniagenes* and 90% SS-10% KC
9	*C.a*-SS:BC10	*C. ammoniagenes* and 90%SS -10% BC

The soils that were completely biocemented were used for Unconfined Compressive Strength tests- UCS (ASTM D 2166-06).

3 RESULTS AND DISCUSSION

3.1 *Characterization of soils*

Silica sand (SS) is a medium-grained sand, lacking plasticity, with a coefficient of uniformity (Cu) of 1.6, a coefficient of curvature (Cc) of 0.87, and is classified by the USCS as poorly graded sand (SP). The FTIR spectrum of SS (Figure 2A), confirmed the presence of quartz (Q), indicated by characteristic absorption bands at 460 cm^{-1}, 511 cm^{-1}, 693 cm^{-1}, 1082 cm^{-1}, 1167 cm^{-1} and the doublet at 779 - 797 cm^{-1} (Dixon 1989). The pH of the SS was 8.5, moderately alkaline, with a point of zero charge (PZC) value of 8 and a low cation exchange capacity (CEC) of 0.24 meq/100g, confirming the neutral electrical charge of SS as a mineral substrate (Soil Science Division Staff 2017).

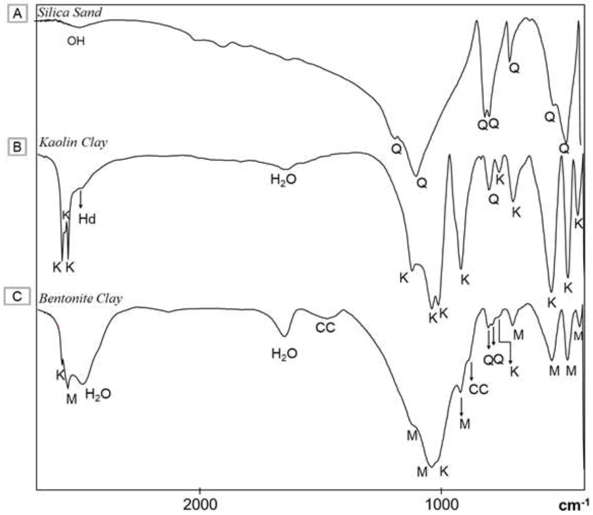

Figure 2. FTIR original samples. a) Silica sand. b) Kaolin. c) Bentonite clay. Note: Q: quartz, k: kaolinite, M: montmorillonite, CC: calcium carbonate, Hd: hydroargillite.

Kaolin (KC) presented a sand fraction of 27.4% and 72.6% of non-plastic fines, classified as low to medium compressibility silt (ML). In the KC FTIR spectrum (Figure 2B), the predominance of kaolinite (K) as a clay mineral was observed (426 cm^{-1}, 469 cm^{-1}, 536 cm^{-1}, 694 cm^{-1}, 910 cm^{-1}, the doublet at 1005 cm^{-1} and 1032 cm^{-1}, 1113 cm^{-1}, 3620 cm^{-1} and 3696 cm^{-1}), mixed with quartz (795 cm^{-1}) and possibly hydroargillite (gibbsite), due to the band at 3458 cm^{-1} (Van Der Marel & Beutelespacher 1976). The pH of KC is 4.1, extremely acidic, with a low CEC (0.50 meq/100 g) similar to SS CEC, but with a PZC of 2.7, suggesting a prevalence of positive electrical charges.

Bentonite clay (BC) had a fines content of 98.4% and a sand fraction of 1.6%. It had a liquid limit (wL) of 427%, a plastic limit (wP) of 52% and a plastic index (PI) of 375%, classified as high plasticity clay (CH). FTIR analysis (Figure 2C) confirmed the presence of montmorillonite (M) as the predominant clay mineral in BC, mixed with a lesser proportion of kaolinite. It is important to note the presence of calcium carbonate (CC) in the BC sample, detected by the broad band at 1460 cm^{-1} and the band at 876 cm^{-1} (Van Der Marel & Beutelespacher 1976). This substrate has a pH of 8.4, moderately alkaline, and a high CEC of 37.7 meq/100 g, almost 40 times higher than SS and KC.

3.2 *Calcium carbonate precipitation bioassay*

3.2.1 pH, DO, Ca

The pH of the liquid medium (Figure 3) exhibited similar trends across different mineral substrates, initially undergoing acidification, followed by subsequent alkalinization until reaching a stable level. The substrate´s influence was evident in both the achieved pH values and the duration of the acidification phase. In the SS and KC samples, the pH reduction phase concluded after 24 h with values of 7.7 and 7.5, respectively. Conversely, in the BC, the acidification phase ended between 24 h and 72 h, with pH levels ranging between 7.2 and 7.5 depending on the microorganism. Subsequently, the pH gradually increased and stabilized around 8.

The DO levels (Figure 4) decreased at the start of the experiment, attributed to increased cellular respiration. Oxygen depletion (0 mg/l) occurred at 24 h in the SS and KC samples, and at 72 h (day 3) in the BC, coinciding with the pH decrease. Subsequently, DO levels recovered after 144 hours (day 6).

The concentration of calcium (Ca) in solution (Figure 5) notably decreased within the first 24 h and exhibited similar patterns in the SS and KC, with Ca availability of 25%, 25% and 60% in the bioassays with *Sporosarcina pasteurii*, *Sutcliffiella cohnii* and *Corynebacterium ammoniagenes*, respectively. The BC displayed lower Ca availability, at 18%, 22% and 42%, respectively. These outcomes corresponded with greater CC precipitation in the BC substrate during the initial 24 h. Additionally, CC precipitation occurred more rapidly with *Sporosarcina pasteurii* and slower with *Corynebacterium ammoniagenes*. The availability of Ca and consequently, CC precipitation, ceased at 72 h (day 3).

In the control samples, both pH and DO, remained relatively constant at their initial values (8.5 y 6.8 mg/l, respectively), throughout the 15-day treatment period, with minor, non-significant fluctuations. The concentration of Ca in solution fluctuated between 85% and 98% in the controls, indicating minimal abiotic precipitation of CC.

3.2.2 Precipitation of calcium carbonate on mineral substrate

Figures 6, 7 and 8 depict the FTIR spectra and the mineral phases present in the SS, KC and BC substrates at the conclusion of the bioassays with *Sporosarcina pasteurii, Sutcliffiella cohnii* and *Corynebacterium ammoniagenes*. The precipitation of CC was evident due to the emergence of new absorption bands that were not present in the soils before the bioassays. These bands, observed between 1420 cm^{-1} and 1480 cm^{-1}, were interpreted as amorphous CC, (ACCν_3) (Andersen & Brecevics 1991), and a well-defined band around 876 cm^{-1}, indicative crystalline CC (CCν_2) (Van Der Marel & Beutelespacher 1976).

The intensity of the crystalline CC bands varies depending on the substrate and the microorganism used. Comparing the band intensity at 876 cm^{-1}, is indicative of the relative amount of precipitated CC. This band exhibited greater intensity in SS and BC and lower intensity in KC.

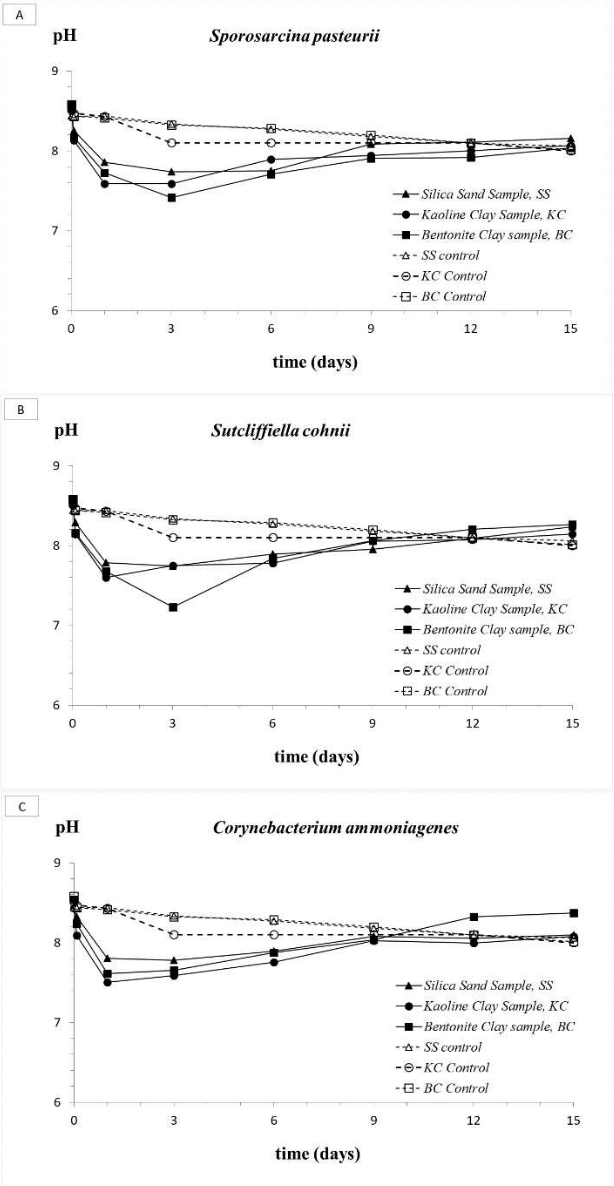

Figure 3. pH liquid medium. a) *Sporosarcina pasteurii.* b) *Sutcliffiella cohnii*. c) *Corynebacterium ammoniagenes*.

Concerning the microorganism, the highest intensity was observed with *Sporosarcina pasteurii* and *Corynebacterium ammoniagenes,* and the lowest intensity with the *Sutcliffiella cohnii* strain. The crystalline CC precipitated in all substrates mainly corresponds to vaterite, Vν_4, as evidenced by the absorption band at 745 cm^{-1} (Andersen & Brecevics 1991).

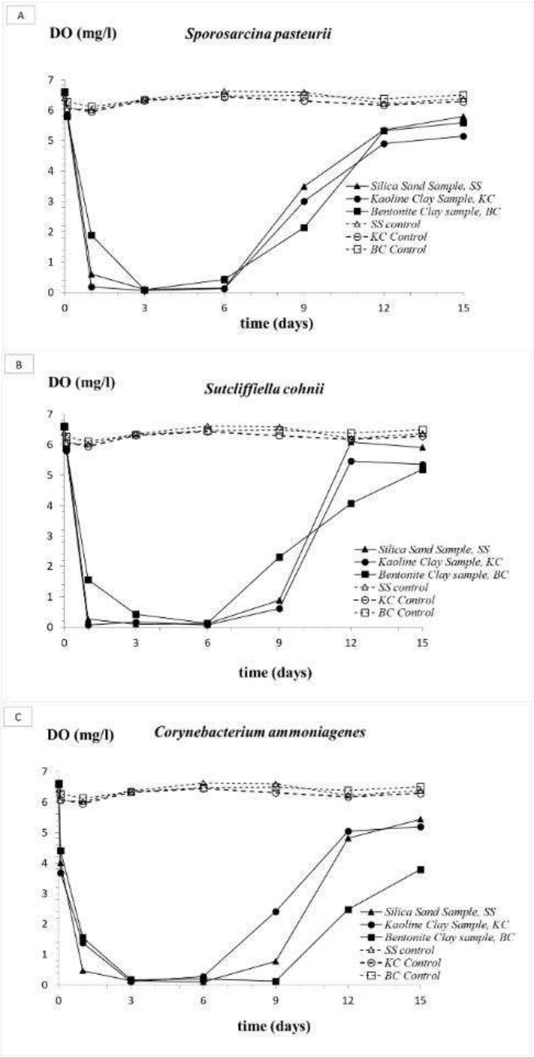

Figure 4. Dissolved oxygen (DO) a) *Sporosarcina pasteurii.* b) *Sutcliffiella cohnii*. c) *Corynebacterium ammoniagenes*.

The SEM images captured after treatment (Figure 9 - 11) depict varied habits and textural associations between the precipitated CC and the mineral substrates.

In the SS with *Corynebacterium ammoniagenes* (Figure 9), the precipitated CC was detected on the surface of the particles, displaying rounded shapes with a botryoidal habit and sizes ranging between approximately 840 nm and 3–6 µm, possibly associated with vaterite.

In the KC with *Sporosarcina pasteurii* (Figure 10) crystals composed of Si, O and Al (associated to kaolinite) were observed intergrown with Ca and C, with some areas showing deposition on the kaolinite particle.

In the SEM image of the BC with *Sutcliffiella cohnii* (Figure 11), a matrix with a petal-shaped texture characteristic of montmorillonite was observed. Some empty spaces were filled with cylindrical shapes, apparently corresponding to calcified bacteria (cb) measuring 10 µm in length. Accumulations of CC with a botryoidal habit, ranging just a few micrometers in diameter (1µm), as well as rhombohedra and/or hexagonal crystals, were also observed.

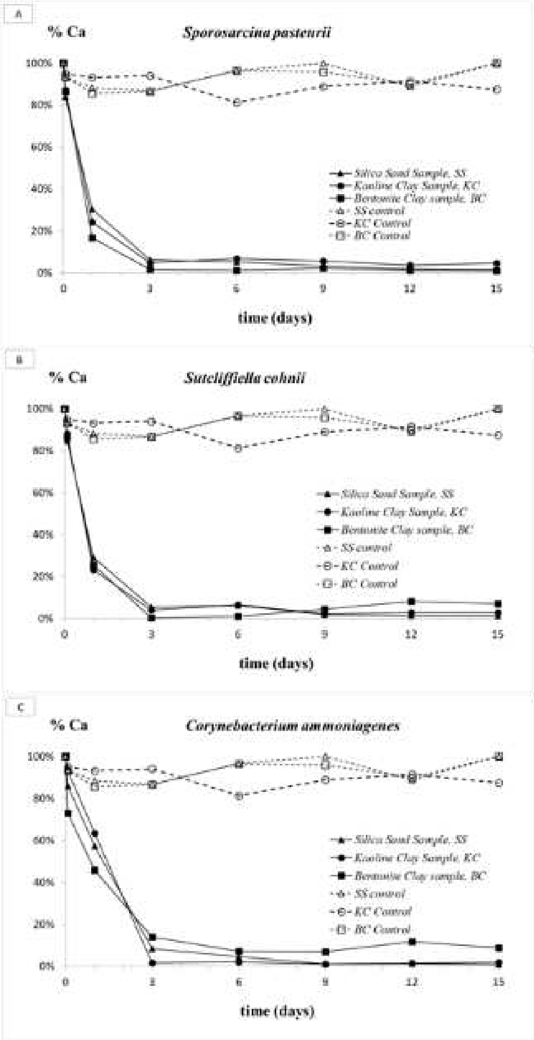

Figure 5. Concentration of calcium (Ca) in solution a) *Sporosarcina pasteurii.* b) *Sutcliffiella cohnii*. c) *Corynebacterium ammoniagenes*.

3.2.3 Quantification of calcium carbonate in soils

The quantification of CC was conducted as gram of CC per gram of soil, expressed as a percentage (See Figure 12). The greatest CC precipitation observed was 22% in the BC sample, while the lowest was 13% in both the SS and KC samples, with not statistically significant differences between them.

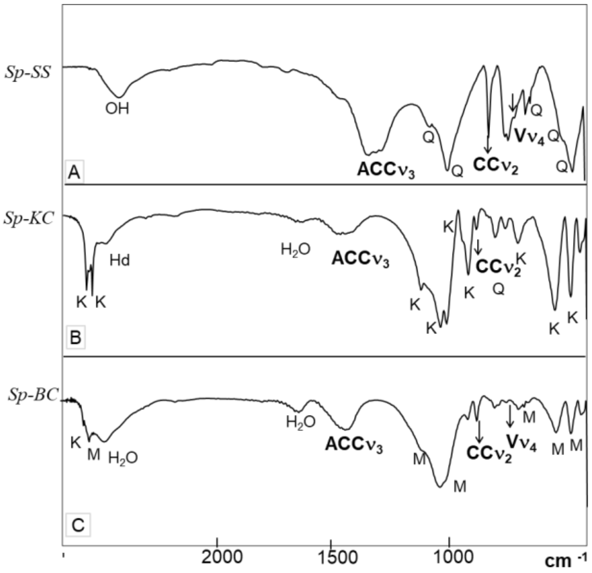

Figure 6. FTIR, *Sporosarcina pasteurii* samples. a) Silica sand. b) Kaolin clay. c) Bentonite clay. Note: Q: quartz, k: kaolinite, M: montmorillonite, Hd: hydroargillite, CC: calcium carbonate, ACC: amorphous calcium carbonate

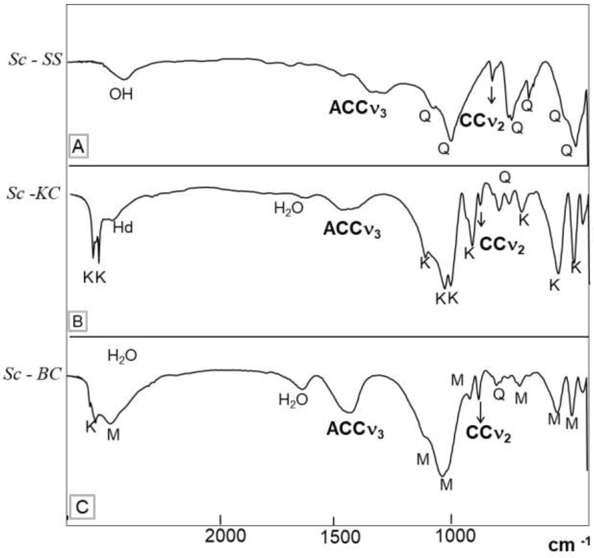

Figure 7. FTIR, *Sutcliffiella cohnii* samples. a) Silica sand. b) Kaolin clay. c) Bentonite clay. Note: Q: quartz, k: kaolinite, M: montmorillonite, Hd: hydroargillite, CC: calcium carbonate, ACC: amorphous calcium carbonate

The affinity of carbonates for bentonite clays, such as montmorillonite and other minerals of the smectite group, has been documented in the literature, from the perspective of the interaction of both minerals (Kralj & Vdovic 2000, Molnár et al. 2019, Fodor et al. 2020). A larger surface area could lead to greater precipitation of CC, as in the case of montmorillonite, which could partly explain the results obtained in the BC.

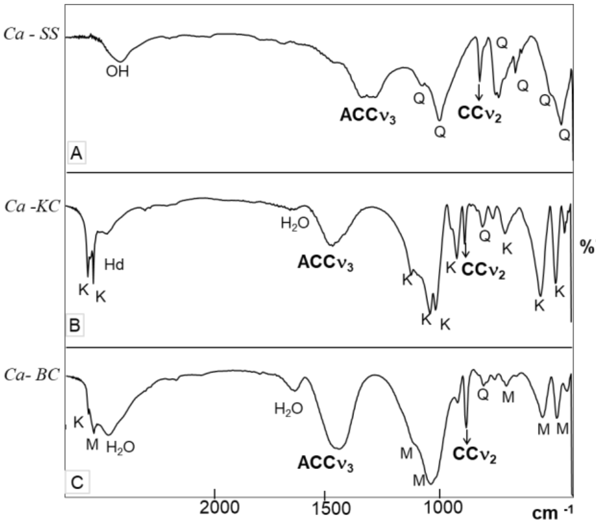

Figure 8. FTIR, *Corynebacterium ammoniagenes* samples. a) Silica sand. b) Kaolin clay. c) Bentonite clay. Note: Q: quartz, k: kaolinite, M: montmorillonite, Hd: hydrargillites, CC: calcium carbonate, ACC: amorphous calcium carbonate

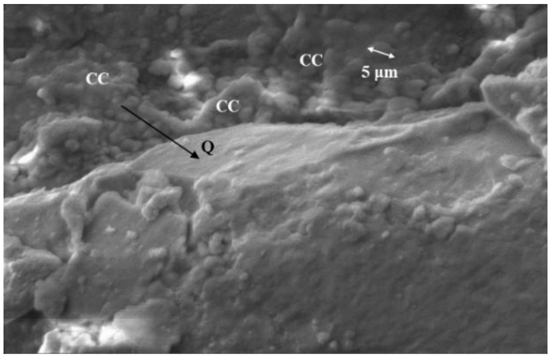

Figure 9. SEM image 2000X (SE, Secondary electron mode) *Corynebacterium ammoniagenes*-Silica Sand. Note: Q = quartz, CC=calcium carbonate.

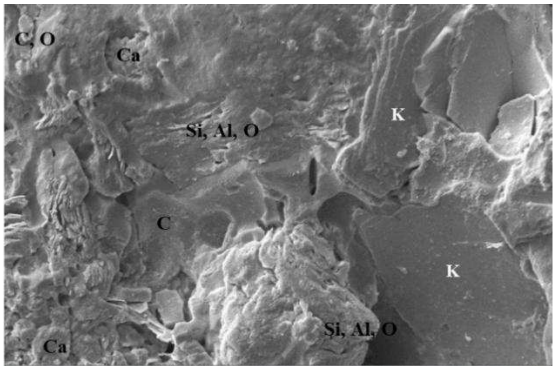

Figure 10. SEM image 750 X (SE, Secondary electron mode), *Sporosarcina pasteurii* – Kaolinite Clay. Note:K= kaolinite, C=carbon, Ca= calcium, Si=silicom, Al=aluminum, O=oxygen.

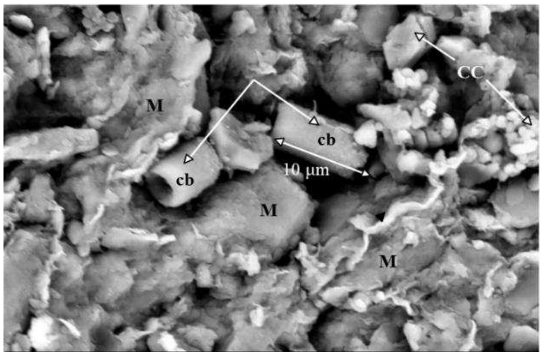

Figure 11. SEM image 2000X (Backscatter electron mode BSE), *Sutcliffiella cohnii* – Bentonite Clay. Note: cb= calcified bacteria, M= montmorillonte, CC=calcium carbonate.

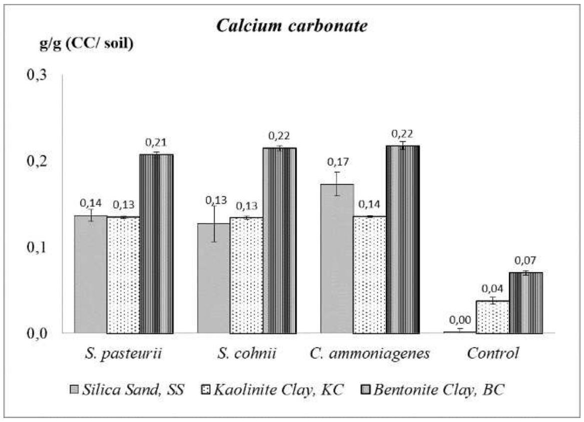

Figure 12. Calcium carbonate content in Erlenmeyers flask

However, according to some researchers (Chen et al. 2017, Zhao et al. 2021), the catalytic effect of montmorillonite on CC precipitation primarily depends on its net negative characteristics, which are not present in kaolinite matrices (with positive charges).

In the KC and BC controls, there was a minor degree of CC precipitation, 4% and 7%, associated with abiotic precipitation. This precipitation can occur due to the intervention of mineral particles as nucleation sites. The difference between the content of biotically and abiotically precipitated carbonate is indicates that the presence of the microorganism catalyzes the CC precipitation reaction.

3.3 Biocemented soils: SS, SS-CK10, SS-BC10

3.3.1 Remaining calcium concentration in solution

For soil biocementation, four successive MICP treatments were administered, each supplying 18.000 mg/l of calcium (Figure 13), for a total of 72.000 mg/l of calcium. Among the treatments, those involving *Sporosarcina pasteurii* proved to be the most effective across all substrates, while those with *Sutcliffiella cohnii* were the least efficient.

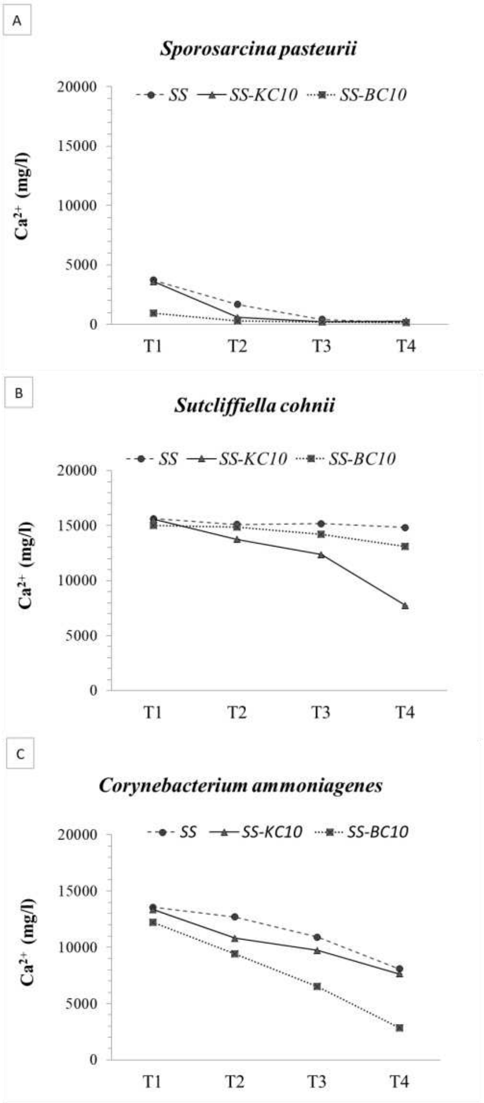

Figure 13. Calcium in solution. a) *Sporosarcina pasteurii*. b) *Sutcliffiella cohnii*. c) *Corynebacterium ammoniagenes*.

At the end of T1 treatments, the smallest remaining calcium concentration in solution was observed in SS-BC10 sample treated with *Sporosarcina pasteurii*, with a Ca in solution of 1000 mg/l, compared to 4000 mg/l in SS and SS-BC10 substrates. From a mineralogical standpoint, the least efficient treatment was observed with SS, suggesting that the presence of 10% BC and 10% KC catalyzed calcium precipitation. It was noted that with each successive treatment, the precipitation process became more efficient, and in the specific case of *Sporosarcina pasteurii* from treatment T3, the Ca supplied is consumed at 100%.

Figure 14 illustrates the accumulated precipitated CC at the end of the four treatments. The precipitated CC was calculated based on the measurement of calcium in solution, revealing the influence of both, the mineral substrate and the microorganism used for MICP on the amount of precipitated CC.

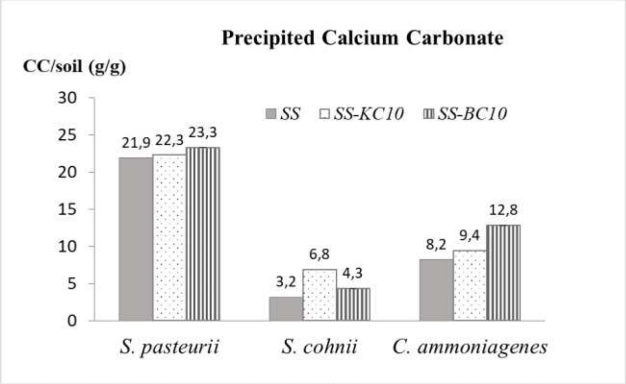

Figure 14. Calcium carbonate content in soil cylinders

3.3.2 Biocemented soil cylinders

Upon demolding the samples after the biological treatment, it was observed that samples *S.p*-SS and *S.p*-SS:KC10 were completely cemented, while sample *S.p*-SS:CB10 was only partially cemented, displaying fragility as it broke into two pieces upon handling (Figure 15a). The soils treated with *Sutcliffiella cohnii* and *Corynebacterium ammoniagenes* exhibited partial cementation (Figure 15b and Figure 15c, respectively). No evidence of cementation was observed in any of the controls samples.

Interestingly, the degree of biocementation observed in the soil cylinders appeared to contradict the amount of CC precipitated. This discrepancy suggests that the quantity of precipitated CC alone is insufficient to achieve optimal biocementation, indicating the presence of other critical variables. The MICP process itself encompasses numerous variables (e.g., types and concentrations of bacteria and reagents), when combined with the diverse intrinsic characteristics of the soil, these factors form a complex network that influences the final outcome. Therefore, relying solely on CC as a measure to characterize the behavior of bio-cemented soils seems inappropriate (Fu et al. 2023). However, some authors (Jiang et al. 2021), mention a minimum CC content of 3% to achieve biocemented samples with sufficient integrity to stand without confinement.

In the case of *S.p*-SS:CB10 sample, a significant portion of the precipitated CC was observed to accumulate in the upper part of the cylinder, forming a 5 mm thick layer without penetrating the soil matrix. This phenomenon may have influenced the biocementation outcome in this sample.

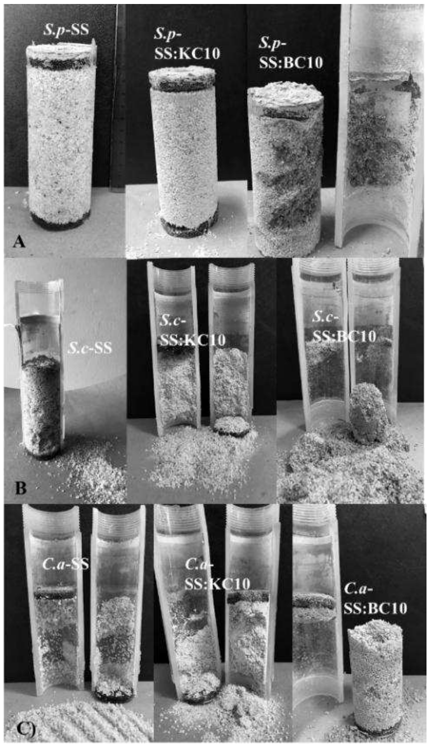

Figure 15. Biocemented soils with a) *Sporosarcina pasteurii*, b) *Sutcliffiella cohnii*, c) *Corynebacterium ammoniagenes*.

3.3.3 FTIR and SEM of Biocemented soils

By using FTIR, CC precipitation was only evident in the tests conducted with *Sporosarcina pasteurii* (Figure 16). However, in the SS: BC10 test, well-defined CC bands were observed at 876 $\mathrm{cm^{-1}}$ (CCv$_2$) and 1424 $\mathrm{cm^{-1}}$ (CCv$_3$), while in the SS and SS:KC10 tests, these bands exhibited very low intensity.

Figure 17A and 17B depict SEM images at 50x and 500x magnification of the SS treated with *Sporosarcina pasteurii*, revealing that the CC covered the sand particles, in some cases, precipitated between them, forming the “bridge” necessary for effective biocementation (Mujah et al. 2017). The crystals have a rhombohedral shape, possibly composed of calcite. Empty spaces between particles were also observed, which were not filled by CC.

Figure 17C shows the SEM images at 100x magnification of *S.p*-SS:KC10. Quartz particles coated with CC, particles exhibiting a planar shape (presumably kaolinite), and CC precipitated in the spaces between the particles without a defined geometric shape were observed.

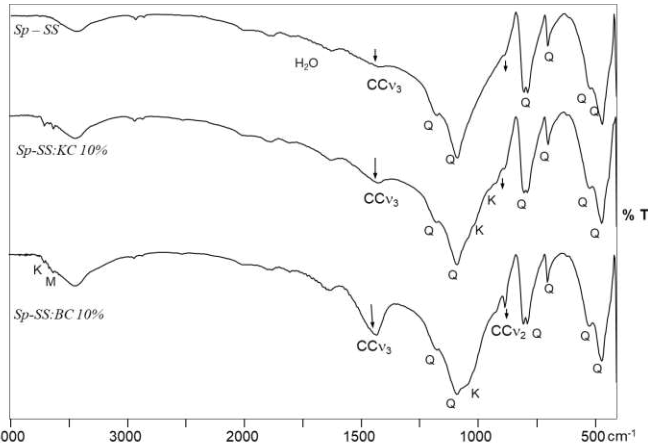

Figure 16. FTIR Biotreated soil with *Sporosarcina pasteurii.*

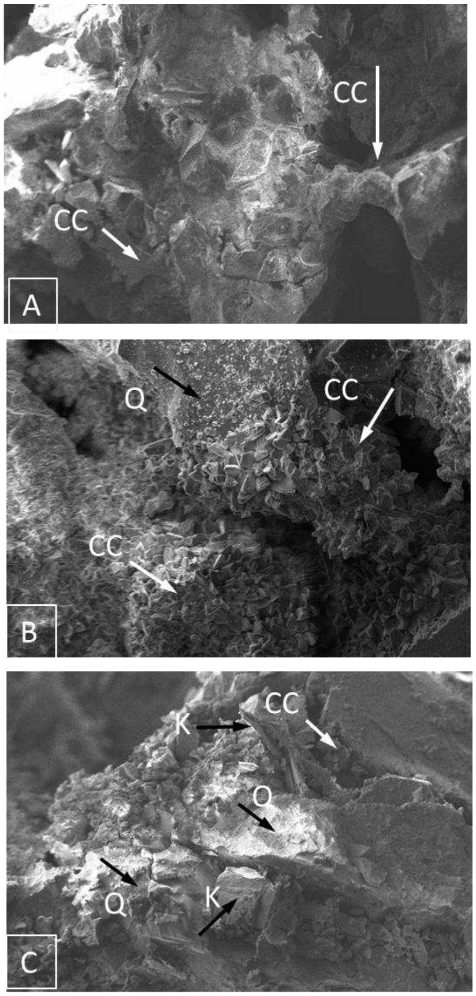

Figure 17. SEM images in Secondary electron mode. a) 54X *S.p* – SS, b) 500X *S.p-* SS. c) 100X *S.p* – SS:KC10. Note: Q = quartz, CC=calcium carbonate, K= kaolinite.

3.3.4 Compressive Strength of biocementing soils

Unconfined compressive strength (UCS) tests were carried out on the samples that were completely biocemented by MICP: *S.p*-SS sample and *S.p*-SS:KC10 sample, a single sample of each soil (Figure 15). The other biotreated soil samples were not fully cemented and fragmented into small pieces. Consequently, they could not undergo testing, similar to the untreated sand sample (SP poorly graded sand), which lacked strength because it was not confined.

The UCS of the *S.p*-SS sample was 934 kPa (Figure 18), exhibiting a failure behavior characteristic of cemented sand (Juárez & Rico 1965, Mitchell 1993, DeJong et al. 2006). The UCS of the *S.p*-SS:KC10 sample was 96 kPa (Figure 19). These UCS values are similar to those obtained by Sotoudehfar et al. (2016) for a SP sand biotreated with *Sporosarcina pasteurii*, which reached UCS values between 296 kPa and 930 kPa. These authors found an increase in strength through MICP compared to the control sample (injection of only a nutrient solution), which reached a UCS value of 85 kPa.

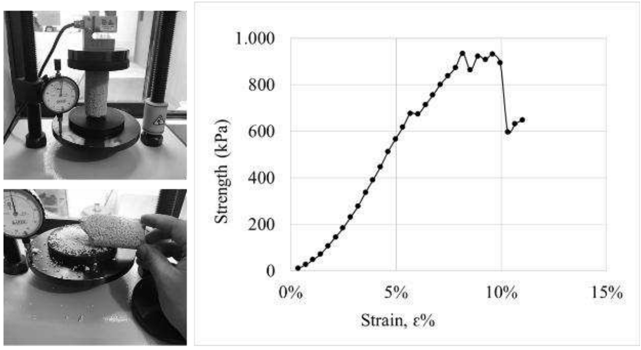

Figure 18. Unconfined compressive strength tests (UCS) *Sporosarcina pasteurii.* – Silica sand sample.

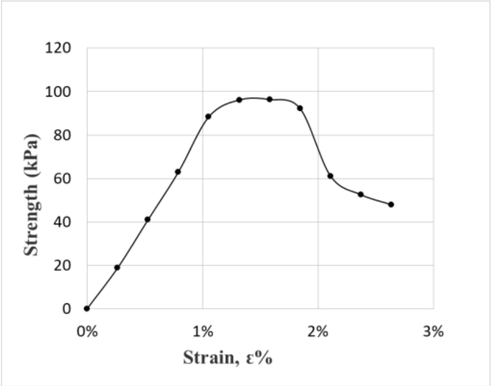

Figure 19. Unconfined compressive strength tests (UCS) *Sporosarcina pasteurii.* – Silica Sand 90%: Kaolinite clay 10% sample.

The UCS test is widely used for assessing the strength of biocemented soils and is considered the most reliable method for evaluating soil stabilization techniques (Ali et al. 1992). Several authors have reported improvements in UCS values for coarse soils treated with MICP (Cheng et al. 2013, Van Paassen 2009, Wang et al. 2018). Most studies agree that the enhanced strength of biocemented soils is primarily attributed to the adhesion of soil grains due to calcium carbonate precipitates filling soil voids (Almajed 2021). This suggests that MICP directly contributes to the cohesion component (Mitchell 1993) of soil strength, thereby increasing undrained cohesion (Sharma & Ramkrishnan 2016).

The strength gain in soils depends on the amount of precipitated calcite. Specifically, to achieve significant improvements in the stiffness and strength of soils treated with biostabilization techniques, a minimum of 4% calcite precipitation per mass of treated soil is required (Park et al. 2014) or 60 kg/m^3 (Whiffin 2004). According to relationships established by some authors between UCS and calcium carbonate content, a UCS value of 900 kPa is associated with calcium carbonate contents ranging from 2% to 9% (Cheng et al. 2013).

4 CONCLUSIONS

The role of mineralogy was prominently evident, particularly in the biogeochemical process of CC precipitation. Variation was observed in the behavior of pH, DO and concentration of Ca in solution over time, depending on whether the mineral substrate is quartz (SS), kaolinite (KC), or montmorillonite (BC).

The precipitation of CC occurs during the acidification period of the medium, starting with a pH of 8.5 and reaching values of 7.2 and 7.5. During this phase, there is a significant reduction in DO and Ca concentration. The BC substrate, composed of montmorillonite, with a negative electrical charge and higher CEC, reached a lower pH value over a longer time (72 h), with a slower decrease in DO and higher Ca consumption, resulting in a greater amount of CC precipitated. In contrast, the SS and KC substrates, with a neutral to positive electrical charge, respectively, exhibited very similar behavior, reaching the minimum pH at 24 h, with a faster decrease in DO but lower Ca consumption and consequently less CC precipitated.

Mineralogy influenced two key aspects: the polymorph and the amount of CC precipitated. The process in BC, although slower, appeared to favor the precipitation of calcite, independently of the microorganism used, while in SS and KC, vaterite was precipitated. However, achieving soil biocementation depends on factors beyond the amount of CC precipitated, and must be studied. The textural association between the particles and CC is crucial for effective biocementation, making it an important control factor for MICP application in geotechnical engineering.

Out of the nine soil samples treated with MICP (Table 1) and their respective controls (soils without application of microorganism), only two samples retained their cylindrical shape upon removal from the mold and were used to assess their mechanical strength. The sample consisting of 100% silica sand achieved a UCS of 934 kPa, while the mixture of 90% silica sand and 10% kaolinite clay reached a UCS of 85 kPa. Both samples were treated with *Sporosarcina pasteurii*, highlighting once more the effectiveness of this microorganism for soil biocementation. These findings confirm that MICP enhances UCS through the adhesion between particles due to calcium carbonate precipitated in the voids of the soil.

5 ACKNOWLEDGEMENTS

The authors are grateful to Laboratory of Biomineralogy and Biohydrometallurgy (Universidad Nacional de Colombia), to the Applied Mineralogy and Bioprocesses research group, to the Politécnico Colombiano Jaime Isaza Cadavid and to Posgrado en Geotecnia de la Universidad de Brasilia (Brasil).

6 REFERENCES

Ali, F.H., Adnan, A. and Choy, C.K. 1992. Geotechnical Properties of a Chemically Stabilized Soil from Malaysia with Rice Husk Ash as an Additive. *Geotech. Geol. Eng*. 10, 117–134.

Almajed, A., Lateef, M.A., Moghal, A.A.B. and Lemboye, K. 2021. State-of-the-Art Review of the Applicability and Challenges of Microbial-Induced Calcite Precipitation (MICP) and Enzyme-Induced Calcite Precipitation (EICP) Techniques for Geotechnical and Geoenvironmental Applications. *Crystals*. 11, 370. https://doi.org/10.3390/cryst11040370

Andersen F.A. and Brecevic L. 1991. Infrared Spectra of Amorphous and Crystalline Calcium Carbonate. *Acta Chem Scand* 45, 1018-1024.

Chen, T., Jiwei L., Peiheng S., Yi L., Jia L., Jian Z., Zuowen H., Tao D., Yongjian D. and Wenkun Z. 2017. Effects of Montmorillonite on the Mineralization and Cementing Properties of Microbiologically Induced Calcium Carbonate. *Advances in Materials Science and Engineering* 7874251, 1-13. https://doi.org/10.1155/2017/7874251.

Cheng L., Cord-Ruwisch R. and Shahin M. A. 2013. Cementation of sand soil by Microbially Induced Calcite Precipitation at various degrees of saturation. *Can. Geotech. J*. 50, 81–90.

DeJong J.T., Fritzges M.B. and Nüsslein K. 2006. Microbial induced cementation to control sand response to undrained shear. *ASCE J. Geotech. Geoenviron. Eng*. 132 (11), 1381–1392.

Dixon J.B. 1989. *Minerals in Soil Environments*. Edited by S.B. Weed. 2nd ed. Madison, WI|USA: Soil Science Society of America Book Series.

Fodor M., Ható Z., Kristóf T. and Pósfai M. 2020. The role of clay surfaces in the heterogeneous nucleation of calcite: Molecular dynamics simulations of cluster formation and attachment. *Chemical Geology* 538, 119497.https://doi.org/10.1016/j.chemgeo.2020.119497.

Fu T., Saracho A.C. and Haigh S.K. 2023. Microbially induced carbonate precipitation (MICP) for soil strengthening: A comprehensive review. *Biogeotechnics* 1, 100002.

Hamilton W.A. 2003. Microbially influenced corrosion as a model system for the study of metal microbe interactions: a unifying electron transfer hypothesis. *Biofouling* 19 (1), 65–76.

Ivanov V. and Jian C. 2008. Applications of microorganism to geotechnical engineering for bioclogging and biocementation of soil in situ. *Reviews in Environmental Science and Biotechnology* 7, 139-153. https://doi.org/10.1007/s11157-007-9126-3.

Jiang N.J., Wang Y.J. and Chu J. 2021. Bio-mediated soil improvement: An introspection into processes, materials, characterization and applications. *Soil Use Manag.* 00, 1–26, https://doi.org/10.1111/sum.12736.

Juárez E. and Rico A. 1965. *Mecánica de suelos*. Tomo I. México.

Kralj D. and Vdović N. 2000. The influence of some naturally occurring minerals on the precipitation of calcium carbonate polymorphs. *Water Research.* 34 (1), 179-184. https://doi.org/10.1016/S0043-1354(99)00110-4.

Lee M. L., Ng W.S. and Tanaka Y. 2013. Stress-deformation and compressibility responses of bio-mediated residual soils. *Ecological Engineering* 60, 142–149. https://doi.org/10.1016/j.ecoleng.2013.07.034.

Mitchell J.K. 1993. *Fundamentals of Soil Behavior*. 2nd ed. Hoboken, N.J|USA: John Wiley and Sons.

Molnár Z., Pósfai M. and Pekker P. 2019. Calcium Carbonate Precipitation Induced by Clay Minerals. *Poster presented at Goldschmidt Conference*, Barcelona|ES, August.

Mujah D., Shahin M.A. and Cheng L. 2017. State-of-the-Art Review of Biocementation by Microbially Induced Calcite Precipitation (MICP) for Soil Stabilization. *Geomicrobiology Journal* 34 (6), 524-537.

Park, S.S., Choi, S.G. and Nam, I.H. 2014. Effect of Plant-Induced Calcite Precipitation on the Strength of Sand. J. *Mater. Civ. Eng.* 26, 06014017.

Sharma, A. and Ramkrishnan, R. 2016. Study on Effect of Microbial Induced Calcite Precipitates on Strength of Fine Grained Soils. *Perspective in Science.* 8, 198–202. https://doi.org/10.1016/j.pisc.2016.03.017

Soil Science Division Staff. 2017. *Soil survey manual: Handbook 18.* Edited by Ditzler, C., K. Scheffe, and H.C. Monger. Washington, DC|USA: United States Department of Agriculture (USDA).

Sotoudehfar, A.R., Sadeghi, M.M., Mokhtari, E. and Shafiei, F. 2016. Assessment of the Parameters Influencing Microbial Calcite Precipitation in Injection Experiments Using Taguchi Methodology. *Geomicrobiology J.* 33 (2) 163–172. https://doi.org/10.1080/01490451.2015.1025316

Van Der Marel H.W. and Beutelespacher H. 1976. *Atlas of Infrared Spectroscopy of Clay Minerals and their Admixtures*. Amsterdam|NL: Elsevier Scientific Pub.

Van Paassen, L.A. 2009. *Biogrout, ground improvement by microbially induced carbonate precipitation*. PhD diss, Department of Biotechnology, Delft University of Technology.

Wang, Z., Zhang, N., Ding, J., Lu, C. and Jin, Y. 2018. Experimental Study on Wind Erosion Resistance and Strength of Sands Treated with Microbial-Induced Calcium Carbonate Precipitation. *Advances in Materials Science and Engineering*. Article ID 3463298, 10 pages. https://doi.org/10.1155/2018/3463298.

Whiffin V. 2004. *Microbial $CaCO_3$ precipitation for the production of biocement*. PhD diss., Murdoch University.

Whiffin V., Van Paassen L. and Harkes M. P. 2007. Microbial carbonate precipitation as a soil improvement technique. *Geomicrobiol. J.* 24 (5), 417–423.

Zhao Y., Zhang P., Fang H., Guo C., Zhang B. and Wang F. 2021. Bentonite-assisted microbial-induced carbonate precipitation for coarse soil improvement. *Bulletin of Engineering Geology and the Environment* 80, 5623–5632. https://doi.org/10.1007/s10064-021-02302-6.

The paper was published in the proceedings of the 17th Pan-American Conference on Soil Mechanics and Geotechnical Engineering (XVII PCSMGE) and was edited by Gonzalo Montalva, Daniel Pollak, Claudio Roman and Luis Valenzuela. The conference was held from November 12th to November 16th 2024 in Chile.